Mathematical and Computer Modelling 50 (2009) 717–725

Contents lists available at ScienceDirect

Mathematical and Computer Modelling

journal homepage: www.elsevier.com/locate/mcm

A cellular automaton model for collective neural dynamics

L. Acedo

Instituto de Matemática Multidisciplinar, Universidad Politécnica de Valencia, Building 8G (2° Floor), Camino de Vera, 46022 Valencia, Spain

ARTICLE INFO

Article history:
Received 3 July 2008
Accepted 12 December 2008

Keywords:
Cellular automata
Epidemic models
Neural networks
Subdiffusive behaviour

ABSTRACT

A stochastic epidemic model for the collective behaviour of a large set of Boolean automata placed upon the sites of a complete graph is revisited. In this paper we study the generalisation of the model to take into account inhibitory neurons. The resulting stochastic cellular automata are completely defined by five parameters: the number of excitatory neurons, N, the number of inhibitory neurons, M, the probabilities of excitation, α, and inhibition, γ, among neurons and the spontaneous transition rate from the firing to the quiescent state, β.

We propose that the background of the electroencephalographic signals could be mimicked by the fluctuations in the total number of firing neurons in the excitatory subnetwork. These fluctuations are Gaussian and the mean-square displacement from an initial state displays a strongly subdiffusive behaviour approximately given by $\sigma^2(t) = A(1-\mathrm{e}^{-t/\tau})$, where $NA = \beta/(\beta+M\gamma)$, $\tau = 2(N\alpha-\beta)$. Comparison with real EEG records exhibits good agreement with these predictions.

1. Introduction

Mathematical models for the dynamical evolution of a set of simple Boolean (or multiple states) automata according to some defined deterministic or stochastic rules have been an area of steady interest since the seminal works of Wolfram [1]. Particularly fecund are the applications to mathematical biology: epidemic spread [2–6], pattern formation and developmental biology [7], or forest-fire models [8]. The last group of models is also generally known as excitable media and they could be traced back to the proposal of Greenberg and Hastings [9]. These models have been also successfully applied to the propagation and breaking of spiral waves in the heart tissue [10]. In sharp contrast with the unremitting effort in so many areas of mathematical biology, the applications of cellular automata to neural networks and the brain are relatively scarce and mostly concentrated on some aspects of brain function, such as memory [11], instead of the global modelling of neural dynamics [12,13]. In this paper we revisit a stochastic cellular automaton in a complete graph that has been recently proposed as a rough model of the brain cortex [14]. In the original version of the model we only considered the counterpart of excitatory neurons whose states could be firing or quiescent. The transitions from the firing state to the resting state, or viceversa, are controlled by two probabilities: the probability that a firing neuron excites one of its quiescent neighbours into the firing state, α, and the rate of spontaneous deactivation of a firing neuron, β. Time is discrete in the model so both probabilities are defined per unit time.

The model exhibits a second-order phase transition with the average fraction of firing neurons playing the role of an order parameter. For $\alpha \leq \alpha_c \approx \beta/N$ (N being the total number of neurons in the network) we found that all neurons are quiescent and the average number of firing neurons starts to rise slowly as α increases over this critical value. However, the variance of the number of firing sites shows a sharp peak for α just above the critical value, α_c, and decays monotonously for larger values of α. In that work we suggested that the statistical behaviour of this simple stochastic network as α decreases could be mapped to a brain in deeper and deeper sleep states. As a preliminary support to this conjecture we compared

E-mail address: luiacrod@imm.upv.es.

0895-7177/$ – see front matter © 2009 Elsevier Ltd. All rights reserved.
doi:10.1016/j.mcm.2008.12.018

the ratio of the statistical deviation of the EEG record in the deep sleep stage (sleep stage 4) with that of awake patients (α rhythm) and we found a good agreement with the prediction of the model for a wide range of parameters $\sigma_{\mathrm{Max}}/\sigma_{\mathrm{Min}} \approx 1.89$. In this scenario, EEG signals are described as the fluctuations in the collective activity of very large clusters of neurons. Some recent physiological studies have revealed that the levels of glutamic acid, the main excitatory neurotransmitter in the cerebral cortex, increase after sleep deprivation in rats [15–18]. The measurements of cerebral glucose utilisation by means of the positron emission tomography technique also reveals a decline in several areas of the brain during sleep [19]. These observations are consistent with a scenario in which the homeostatic equilibrium of neurotransmitters is different between sleep states and the awake state and could be mimicked by adjustments of the probabilities in our model.

The original version of our model only considered Boolean automata at every site of a complete graph corresponding to excitatory neurons. It is a well-known fact that about a 20% of cortical neurons are inhibitory [20], their primary role being to avoid overexcitation of the cortex. Consequently, in this paper we generalise our stochastic Boolean cellular automaton by including a fraction of inhibitory sites in the complete graph. If the automata at these sites are in the firing state, they can inhibit any of its firing neighbours with a probability γ per time-step. We also observe a second-order phase transition for this generalised model but the variance exhibits a richer dependence with α. Moreover, the average number of firing neurons is reduced in the excitatory subnetwork as expected from an interaction with the inhibitory sites but, remarkably, the critical point, α_c, keeps the same and does not depend on γ. So, a nice first prediction of the excitatory-inhibitory model is that inhibitory neurons could reduce the excitation of the cortex, as neurophysiology tells us, but they can never prevent the cortex from working, i.e., they never reduce the excitation to zero. As inhibition is taking into account, we find that fluctuations are larger than in purely excitatory networks. The distribution of these fluctuations are gaussian as expected and they are approached subdiffusively. Subdiffusive behaviour is also found in disordered systems and fractals [21] and arise from the random walk of particles in the convoluted structure of these substrates [22]. In our case, the mean-square displacement reaches a plateau and we could parallel this behaviour with the subdiffusion of a particle in a closed domain. The comparison of the mean-square displacement obtained from large sequences of EEG will confirm that these signals also manifest this kind of confinement. This will strengthen our thesis that EEG is, to some extent, a statistical epiphenomenon derived from the collective interactions of large networks of neurons.

The structure of the paper is as follows: In Section 2 we define the model and describe the updating rules for the cellular automata, the corresponding Markovian evolution equations for the average number of firing neurons are derived and a stability analysis of the critical points is performed. The distribution of small fluctuations around the stable critical point is derived in Section 3. In this section we also calculate the mean-square displacement for the time series composed by the fraction of firing neurons in both subnetworks and analyse the second-order phase transition exhibited by the model. Statistical analysis of real EEG records is performed in Section 4 and compared with the functional forms predicted in the previous section. The paper ends with some concluding remarks in Section 5.

2. Cellular automaton model and Markovian evolution equations

Our model is defined as a set of $N+M$ Boolean automata in a complete graph. These automata are placed upon the vertices of the graph with the edges mimicking neural synapses among them. The complete graph topology has already been used both in comparative neuroanatomy [24] and neural networks [11] and could be a reasonable description of compartments containing the square root of the total number of neurons in the brain [24]. As suggested by the partition we have made, the number N represents the excitatory automata neurons and $M < N$ are the inhibitory ones. Both kinds of neuron are found in any of two states: firing or resting. Time is assumed to be discrete and dynamical evolution proceeds according to the following stochastic rules: (i) The transition resting $\to$ firing takes place with a probability α per unit time if the resting neuron is connected with a single firing excitatory neuron. Taking into account that all sites are connected, and assuming the statistical independence of the influences exerted by the excitatory firing neurons on the resting one, we have that the probability for a given quiescent neuron to become firing is $1-(1-\alpha)^E$, where E is the number of firing excitatory neurons in the previous time-step. (ii) The transition firing $\to$ resting happens in two ways: spontaneously (with a probability β) or by the influence of the firing inhibitory neurons with a probability γ per unit time. So, the global probability for this transition is $1-(1-\gamma)^I(1-\beta)$, where I is the total number of inhibitory automata in the firing state. These rules are, of course, somewhat arbitrary but they have been chosen as a simpler way to incorporate inhibition into the model.

We denote as $E(t)$, $I(t)$ the number of excitatory and inhibitory automata in the firing state at time step t, respectively. The rules lead easily to the following Markovian evolution equations:

$$\begin{aligned} E(t+1) &= E(t) + \left(1-(1-\alpha)^{E(t)}\right)(N-E(t)) - \left(1-(1-\gamma)^{I(t)}(1-\beta)\right)E(t) \\ I(t+1) &= I(t) + \left(1-(1-\alpha)^{E(t)}\right)(M-I(t)) - \left(1-(1-\gamma)^{I(t)}(1-\beta)\right)I(t). \end{aligned} \tag{1}$$

We now define the fractions of firing excitatory neurons, $x(t) = E(t)/N$, and firing inhibitory neurons, $y(t) = I(t)/M$, and the corresponding evolution equations become:

$$\begin{aligned} x(t+1) &= x(t) + f(x, y, \alpha, \beta, \gamma, N, M) \\ y(t+1) &= y(t) + g(x, y, \alpha, \beta, \gamma, N, M), \end{aligned} \tag{2}$$

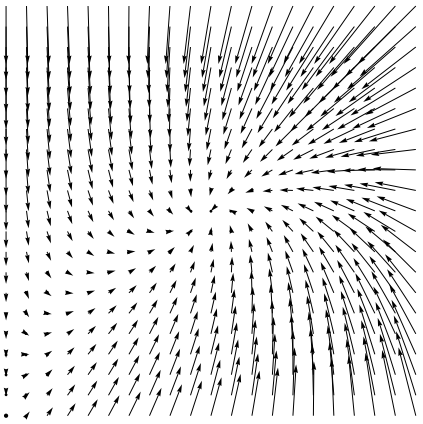

Fig. 1. Vector field $(f(x, y), g(x, y))$ for $\alpha = 0.0005$, $\beta = 0.1$, $\gamma = 0.001$, $N = 100$ and $M = 300$. The non-trivial critical point is at $x_0 = y_0 \simeq 0.4943$ while $x_0 = y_0 = 0$ is at the bottom left.

where

$$\begin{aligned} f(x, y, \alpha, \beta, \gamma, N, M) &= (1 - x)\left(1 - (1 - \alpha)^{Nx}\right) - \left(1 - (1 - \beta)(1 - \gamma)^{My}\right) x \\ g(x, y, \alpha, \beta, \gamma, N, M) &= (1 - y)\left(1 - (1 - \alpha)^{Nx}\right) - \left(1 - (1 - \beta)(1 - \gamma)^{My}\right) y. \end{aligned} \tag{3}$$

Critical points are found by equating both functions to zero which leads to the condition $x_0 = y_0$, the fraction of firing neurons is the same in the excitatory subnetwork and the inhibitory one. The value of x_0 verifies the transcendent equation:

$$(1 - x_0)\left(1 - (1 - \alpha)^{Nx_0}\right) = \left(1 - (1 - \beta)(1 - \gamma)^{Mx_0}\right) x_0. \tag{4}$$

The trivial solution $x_0 = 0$ corresponds to a stationary state in which every neuron is resting. It can be shown [14] that a second critical point appears for $\alpha > \alpha_c$ where:

$$\alpha_c = 1 - \mathrm{e}^{-\beta/N}. \tag{5}$$

In the limit $N\alpha \ll 1$, $M\gamma \ll 1$ and $\beta \ll 1$ we can solve Eq. (4) approximately by linearisation and we get:

$$x_0 = y_0 \simeq \frac{\alpha - \alpha_c}{\alpha + M\gamma/N}, \quad \alpha > \alpha_c = \beta/N, \tag{6}$$

where we have approximated Eq. (5) for small β. Surprisingly, the inhibitory probability, γ, has no influence on the critical threshold for α but, as expected, their presence diminishes global excitation above the threshold. Consequently, we find that inhibitory neurons can modulate the excitation but they cannot drive it to zero. We must notice that in order to avoid probability overcounting (neurons excited several times at the same time-step) one must derive Eq. (1) from a master equation of the system as a whole [25]. This approach implies that $\alpha_c = \beta/N$ but it is not too drastic a change if transition probabilities are small.

A standard linear stability analysis shows us that the trivial critical point, $x_0 = y_0 = 0$ is a stable node for $\alpha < \alpha_c$ (the eigenvalues of the matrix of the linearised system around this point are: $\lambda_1 = -\beta$ and $\lambda_2 = -\beta - N\ln(1 - \alpha)$) and we know that this is the single critical point in that regime [14]. For $\alpha > \alpha_c$ a bifurcation occurs and $x_0 = y_0 = 0$ becomes an unstable saddle point while the new critical point is a stable node. To illustrate this transition we have plotted a flow diagram of vectors $(f(x, y), g(x, y))$ in Fig. 1. With the parameters we have chosen the stable critical point is approximately at the center of the diagram. The approach we have developed in this section is only a mean-field theory. For the rest of the paper we will consider that the system have settled at the stable critical point and we will study the random excursions around it.

3. Propagator and subdiffusive dynamics

In this section we analyse the statistical dynamics of the model through the definition of the discrete distribution of firing neurons. We will denote by $p_{n,t}$ the probability of finding n excitatory neurons in the firing state. Analogously, $q_{m,t}$ is the corresponding probability for the inhibitory sites. We will also find it convenient to define the global activation and deactivation probabilities as follows:

$$\begin{aligned} A(\alpha, n) &= 1 - (1 - \alpha)^n \\ G(\beta, \gamma, m) &= 1 - (1 - \beta)\,(1 - \gamma)^m. \end{aligned} \tag{7}$$

A detailed balance of the sites that change their state from time step t to time step $t+1$ yields the coupled evolution equations for the distributions of both kinds of firing neurons:

$$\begin{aligned} p_{n',t+1} &= \sum_{n=0}^{N}\sum_{m=0}^{M} p_{n,t}q_{m,t}\sum_{l=0}^{n}\sum_{j=0}^{N-n}\delta_{n-l+j,n'}\,\mathcal{P}_n\left(G(\beta,\gamma,m),l\right)\mathcal{P}_{N-n}\left(A(\alpha,n),j\right) \\ q_{m',t+1} &= \sum_{n=0}^{N}\sum_{m=0}^{M} p_{n,t}q_{m,t}\sum_{l=0}^{m}\sum_{j=0}^{M-m}\delta_{m-l+j,m'}\,\mathcal{P}_m\left(G(\beta,\gamma,m),l\right)\mathcal{P}_{M-m}\left(A(\alpha,n),j\right), \end{aligned} \tag{8}$$

where $\mathcal{P}_N(\mu,k) = \binom{N}{k}\mu^k(1-\mu)^{N-k}$ is the binomial distribution for k positive results out of N total attempts if every positive result is obtained with probability μ. Discrete equations are too complicated for further analytic treatment so we have taken the continuous limit in which n, m, N and M tend to infinity but the fractions $x = n/N$ and $y = m/M$ remains finite. This approach readily yields a system of integral equations:

$$\begin{aligned} p(x,t+1) &= \int_{-\infty}^{\infty}\int_{-\infty}^{\infty} \mathrm{d}z\,\mathrm{d}v\,p(z,t)q(v,t)\mathcal{K}(z,v;x) \\ q(y,t+1) &= \int_{-\infty}^{\infty}\int_{-\infty}^{\infty} \mathrm{d}z\,\mathrm{d}v\,p(z,t)q(v,t)\mathcal{L}(z,v;y). \end{aligned} \tag{9}$$

The limits of integration have been extended to infinity to keep the problem amenable to analytic treatment. The errors introduced by this substitution of the limits are small because the kernels, as we see below, are exponentially small as the arguments tend to infinity. The transition rates appearing as kernels in Eq. (9) are explicitly defined in terms of integrals over the fraction of firing neurons which become quiescent as follows:

$$\begin{aligned} \mathcal{K}(z,v;x) &= \int_{-\infty}^{\infty}\mathrm{d}u\,\mathcal{P}_{z,N}\left(G(\beta,\gamma,Mv),u\right)\mathcal{P}_{1-z,N}\left(A(\alpha,Nz),x+u-z\right) \\ \mathcal{L}(z,v;y) &= \int_{-\infty}^{\infty}\mathrm{d}u\,\mathcal{P}_{v,M}\left(G(\beta,\gamma,Mv),u\right)\mathcal{P}_{1-v,M}\left(A(\alpha,Nz),y+u-v\right), \end{aligned} \tag{10}$$

where the binomial distributions are replaced by their gaussian limits:

$$\mathcal{K}(z,v;x) = \sqrt{\frac{N}{2\pi g(z,v)}}\,\mathrm{e}^{-N(x-z-f(z,v))^2/(2g(z,v))}, \tag{11}$$

and a similar expression for $\mathcal{L}(z,v;x)$ where M appears instead of N. The functions $f(z,v)$ and $g(z,v)$ are given by:

$$\begin{aligned} f(z,v) &= (1-z)A(\alpha,Nz) - zG(\beta,\gamma,Mv) \\ g(z,v) &= zG(\beta,\gamma,Mv)\left(1-G(\beta,\gamma,Mv)\right) + (1-z)A(\alpha,z)\left(1-A(\alpha,z)\right). \end{aligned} \tag{12}$$

Because of the nonlinear dependence of the functions in Eq. (12) on the fractions of firing neurons we have non-gaussian transition rates. Those kernels are still too intricate in order to find exact solutions of the system of integral equations in Eq. (9). But, as we are interested in small fluctuations around the stationary state given by Eq. (6), we finally turn to a perturbation approach and define the linearised transition rates as follows:

$$\begin{aligned} \kappa_N(\epsilon,\delta;\mu) &= \mathcal{K}(x_0+\epsilon,x_0+\delta;x_0+\mu) \\ \kappa_M(\epsilon,\delta;\mu) &= \mathcal{L}(x_0+\epsilon,x_0+\delta;x_0+\mu), \quad \epsilon,\delta,\mu \ll 1, \end{aligned} \tag{13}$$

From Eqs. (7), (10) and (11) we get:

$$\kappa_N(\epsilon,\delta;\mu) = \sqrt{\frac{N}{2\pi g(x_0,x_0)}}\,\mathrm{e}^{-(N/2)(\mu-\epsilon c(x_0)-\delta d(x_0))^2/g(x_0,x_0)}, \tag{14}$$

with

$$\begin{aligned} c(x_0) &= (1-\alpha)^{Nx_0}\left(1-N(1-x_0)\ln(1-\alpha)\right) + (1-\beta)(1-\gamma)^{Mx_0} - 1 \\ d(x_0) &= (1-\beta)Mx_0(1-\gamma)^{Mx_0}\ln(1-\gamma). \end{aligned} \tag{15}$$

The perturbation propagators for the excitatory and inhibitory subnetworks are now denoted by $\bar{p}(\mu,t)$ and $\bar{q}(\nu,t)$, respectively. They are defined as the probabilities of finding a small difference, μ or ν, from the fraction of firing neurons in the stationary state at time t if we start with the fraction of firing neurons $x_0 = y_0$ given in Eq. (6) at $t = 0$. The corresponding evolution equations are written in parallel with those in Eq. (9) yielding:

$$\begin{aligned} \bar{p}(\mu,t+1) &= \int_{-\infty}^{\infty}\mathrm{d}\mu_1\int_{-\infty}^{\infty}\mathrm{d}\nu_1\bar{p}(\mu_1,t)\,\bar{q}(\nu_1,t)\,\kappa_N(\mu_1,\nu_1;\mu) \\ \bar{q}(\nu,t+1) &= \int_{-\infty}^{\infty}\mathrm{d}\mu_1\int_{-\infty}^{\infty}\mathrm{d}\nu_1\bar{p}(\mu_1,t)\bar{q}(\nu_1,t)\kappa_M(\mu_1,\nu_1;\nu). \end{aligned} \tag{16}$$

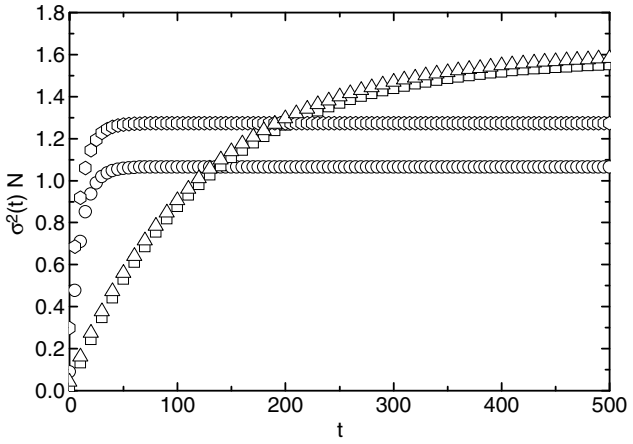

Fig. 2. The variance of the fraction of firing automata representing both the excitatory and inhibitory neurons versus time. We have considered a network with $N = 1000$, $M = 300$, $\beta = 0.1$ and $\gamma = 0.01$. The excitation probabilities are $\alpha = 0.0005$ (circles for excitatory sites and hexagons for the inhibitory sites) and $\alpha = 0.0002$ (squares and triangles for the excitatory and the inhibitory sites, respectively).

If we now take a Dirac delta initial condition: $\bar{p}(\mu, t) = \delta(\mu)$, $\bar{q}(\nu, t) = \delta(\nu)$, the system of coupled integral equations in Eq. (16) can be easily solved by the iteration of the convolution of gaussians. Obviously the result are Gaussian propagators:

$$\bar{p}(\mu, t) = \frac{1}{\sqrt{2\pi\sigma^2(t)}}\, \mathrm{e}^{-\mu^2/(2\sigma^2(t))}, \qquad \bar{q}(\mu, t) = \frac{1}{\sqrt{2\pi\hat{\sigma}^2(t)}}\, \mathrm{e}^{-\mu^2/(2\hat{\sigma}^2(t))}, \tag{17}$$

where the time-dependent variances are obtained by the iteration of the following system:

$$\begin{aligned} \sigma^2(t+1) &= \frac{g(x_0, x_0)}{N} + c^2(x_0)\sigma^2(t) + d^2(x_0)\hat{\sigma}^2(t) \\ \hat{\sigma}^2(t+1) &= \frac{g(x_0, x_0)}{M} + c^2(x_0)\sigma^2(t) + d^2(x_0)\hat{\sigma}^2(t), \end{aligned} \tag{18}$$

with the initial conditions $\sigma^2(t = 0) = \hat{\sigma}^2(t = 0) = 0$. In order to grasp the time dynamics described by Eq. (18) we have plotted in Fig. 2 the result of the numerical iteration of the system for some typical parameters. In particular, we have considered two values of α slightly above the critical threshold. We observe that the fluctuations on the number of firing neurons in the inhibitory subnetwork are larger than those of the excitatory one. Nevertheless, the relative difference between the variances shrinks as we approach the threshold $\alpha \to \alpha_c^+$.We will interpret the excursions performed by the number of firing neurons as a random walk, the relevant quantity characterising this process is the mean-square displacement [21,22] defined as $\langle (x(t) - x_0)^2 \rangle = \sigma^2(t)$, where x_0 is the average fraction of firing sites in the stationary state and $\sigma^2(t)$ is the variance in Eq. (18). It is clear from Fig. 2 that the behaviour is strongly subdiffusive. Taking into account that a plateau is reached in a short time, the evolution of the variance should be compared with that of the mean-square displacement of a set of random walkers in a closed domain. It is also remarkable that the plateau corresponds to larger values of the variance and the dynamics is slower as $\alpha \to \alpha_c^+$. Similar results are found if we only consider excitatory neurons [14]. In Fig. 3 we have also plotted the variance of the final stationary distribution obtained after a sufficiently large number of iterations of Eq. (18) as a function of α while the remaining parameters are kept fixed. A sharp peak is found just above the critical threshold, this is followed by a fast decrease towards a minimum and a final plateau is reached for larger values of α. Notice that in the case of the purely excitatory model this function decreases monotonously above the critical threshold. From Eqs. (7), (12) and (15) we can evaluate the following approximations in the limit $\alpha \to \alpha_c^+$, $\beta \ll 1$ and $M\gamma \ll 1$:

$$\begin{aligned} c(x_0) &= 1 - N(\alpha - \alpha_c) + \mathcal{O}\left((\alpha - \alpha_c)^2\right) + \mathcal{O}\left(M\gamma(\alpha - \alpha_c)\right) \\ d(x_0) &= \mathcal{O}\left(M\gamma(\alpha - \alpha_c)\right) \\ g(x_0) &= \frac{2N\beta}{\beta + M\gamma}(\alpha - \alpha_c) + \mathcal{O}\left((\alpha - \alpha_c)^2\right). \end{aligned} \tag{19}$$

By ignoring second-order terms, the last addend of the iteration system in Eq. (18) can be removed and the first equation of the system becomes independent of the second. The resulting series is geometrical and is readily added to give:

$$\sigma^2(t) = \frac{g(x_0)}{N}\frac{1 - c(x_0)^{2t}}{1 - c^2(x_0)} \simeq \frac{\beta}{N(\beta + M\gamma)}\left(1 - \mathrm{e}^{-t/\tau}\right) \tag{20}$$

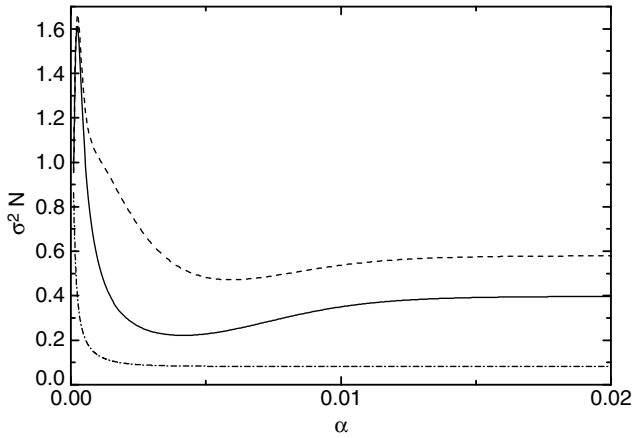

Fig. 3. The variance of the fraction of firing neurons versus α for a network with $N = 10^3$, $M = 300$, $\beta = 0.1$ and $\gamma = 0.01$ for the excitatory subnetwork (solid line) and the inhibitory subnetwork (dashed line). The dashed-dotted line is the result for the purely excitatory model with $N = 1000$ and $\beta = 0.1$.

$$\begin{aligned}\hat{\sigma}^2(t) &= \frac{g(x_0)}{M} + c^2(x_0)\frac{g(x_0)}{N}\frac{1-c(x_0)^{2(t-1)}}{1-c^2(x_0)} \\ &\simeq \frac{2N\beta}{M(\beta+M\gamma)}(\alpha-\alpha_c) + \frac{\beta}{N(\beta+M\gamma)}\left(1-N(\alpha-\alpha_c)\right)\left(1-\mathrm{e}^{-(t-1)/\tau}\right),\end{aligned} \tag{21}$$

where $\tau = 1/(2N(\alpha-\alpha_c))$. Taking the limit $t \to \infty$ we get the critical behaviour of the variances of the fraction of firing neurons in the excitatory and inhibitory subnetworks as follows:

$$\sigma^2 = \begin{cases} 0 & 0 \le \alpha \le \alpha_c \\ \dfrac{1}{N}\dfrac{\beta}{\beta+M\gamma} & 0 < \alpha-\alpha_c \ll 1, \end{cases} \tag{22}$$

$$\hat{\sigma}^2 = \begin{cases} 0 & 0 \le \alpha \le \alpha_c \\ \dfrac{1}{N}\dfrac{\beta}{\beta+M\gamma} + 2\dfrac{(N/M-1)\beta}{\beta+M\gamma}(\alpha-\alpha_c) & 0 < \alpha-\alpha_c \ll 1. \end{cases} \tag{23}$$

According to Eqs. (22) and (23) we have $\lim_{\alpha\to\alpha_c^+}\sigma^2 = \lim_{\alpha\to\alpha_c^+}\hat{\sigma}^2$ as already have been observed in Figs. 2 and 3. The finite jump of the variance at the critical threshold also allows us to classify this transition as second-order.

4. Statistical analysis of EEG

In this section we will discuss some statistical analysis we have performed on real time series of electroencephalographic (EEG) records inspired by our model. EEG is a non-invasive technique with a long tradition in clinical neurology in which brain electrical activity is recorded by means of a set of electrodes attached to the scalp with adhesive materials [26]. In this technique the tiny voltage differences between pair of electrodes are amplified and registered with a temporal resolution ∼4 ms. Striking differences are found among the EEG of an awake normal subject (we have an alpha rhythm in this case which is characterised by its low amplitude and frequencies in the range 8–12 Hz) and that of deep sleep, also known as sleep stage 4 (delta waves, approximately two times the amplitude of the alpha rhythm and with average frequencies in the range of 2 Hz). For the reason of its small frequency, the deepest phase of sleep also receives the name of slow wave sleep. It is generally accepted that some subcortical structures in the brain, such as the thalamus or the brainstem, could play the role of pacemakers for some rhythms. However, EEG is far from being periodic. Moreover, EEG is the most complex physiological signal and it does not seem strangely odd to hypothesise a statistical origin for the EEG background. This would imply that general statistical properties of the fluctuations in network models could be mapped to some aspects of the real EEG. To test this idea, we will establish a correspondence between the time-dependent variance of the fluctuations in the excitatory subnetwork of the model and the mean-square displacement of cortical EEG signals as follows:

$$\begin{aligned}\left\langle (V(t)-V_0)^2 \right\rangle &= N^2\rho^2\sigma^2(t) = \frac{N\beta}{\beta+M\gamma}\rho^2\left(1-\mathrm{e}^{-t/\tau}\right), \\ \tau &= \frac{1}{2N\alpha-\beta},\end{aligned} \tag{24}$$

where ρ denotes the contribution of a single neuron to the global electric potential integrated at the electrodes in the EEG protocol. In order to test the validity of this model we have studied two EEG records from the same subject [27]: One of them

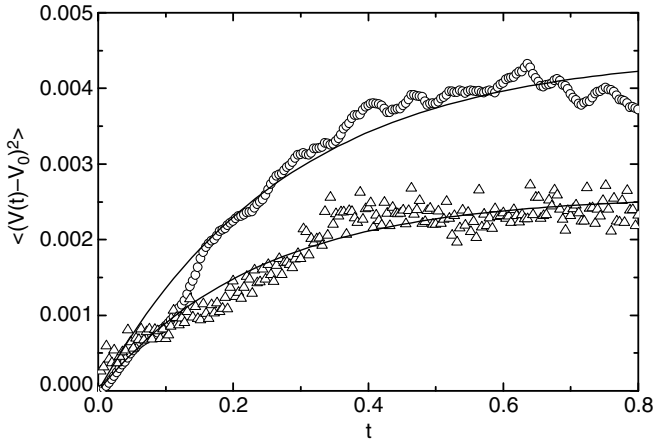

Fig. 4. Mean-square displacement for sleep stage 4 EEG (circles) and alpha rhythm (triangles). Solid lines are non-linear Box-Lucas fits [23] by Eq. (24) as explained in the main text.

corresponding to the waking state and consisting of six minutes of alpha rhythm sampled every 4 ms and the other consisting of a four minute record of delta rhythm. These records were divided in portions of 1 second each and the mean-square displacement from the initial value of the voltage was calculated for every portion and, finally, averaged over all portions. Results are plotted in Fig. 4 We have found that a nonlinear fit by the simple functional form in Eq. (24) is relatively good (reduced $\chi^2 < 5 \times 10^{-8}$, correlation coefficient $R^2 > 0.92$ in both cases). The time scales are $\tau_\delta = 0.23(1)$ and $\tau_\alpha = 0.28(1)$ seconds for the delta and the alpha rhythms, respectively. In order to perform this fitting we have taken $N = 10\,000$ neurons in the excitatory subnetwork, $M = 2000$ inhibitory neurons, $\rho = 1$ mV, and consider equal probabilities of excitation and inhibition, $\alpha = \gamma$. With these conditions we restrict to a two-parameter fit obtaining: $\alpha = \gamma = 2.15 \times 10^{-4}$, $\beta = 0.35$ for the delta rhythm, and $\alpha = \gamma = 2.3 \times 10^{-4}$, $\beta = 0.16$ for the alpha rhythm. Of course, these are not the only or the best parameters to achieve the fitting of the experimental signals. Notwithstanding this arbitrariness, it is remarkable that we can obtain sensible probabilities only for a reasonable choice for the number of neurons and the electric potential scale, ρ. Moreover, the fact that the curves in Fig. 4 do not cross suggests that we cannot keep β and γ fixed as α varies in other to obtain the relative behaviour of EEG signals in different states (See Fig. 2). A better scenario would be obtained by keeping the excitatory probability, α, and the inhibitory probability, γ, fixed, and almost coincident, while the spontaneous deactivation probability increases as sleep proceeds to deeper and deeper states. We have also plotted in Fig. 5 the histograms of both EEG records. In order to get them we have classified the full EEG records into bins of 0.005 mV. Our stochastic cellular automaton model predicts a Gaussian stationary distribution for the fluctuations of the fraction of firing neurons, as given in Eq. (17), so we have fitted these histograms to gaussians. The agreement is also good (reduced $\chi^2 < 10^{-5}$, with a correlation coefficient $R^2 > 0.96$). Gaussian distributions for noisy signals are ubiquitous and, consequently, we cannot consider, by any means, this as a strong prediction of stochastic network models. Nevertheless, Fig. 5 makes evident the different amplitude of the EEG signals recorded from subjects in the waking and the deep sleep states. The width for the slow wave sleep signal is $\sigma_{\mathrm{SWS}} = 0.071(2)$ while for the α rhythm we have $\sigma_{\mathrm{AWAKE}} = 0.0386(7)$. The ratio between the variances:

$$\frac{\sigma^2_{\mathrm{SWS}}}{\sigma^2_{\mathrm{AWAKE}}} = 3.4(1), \tag{25}$$

is known to be a general feature of the EEG of normal subjects [14]. The ratio in Eq. (25) between the variances of the signals with the largest amplitude and those with the lowest amplitude produced by a normal brain seems a more stringent parameter for testing the validity of stochastic cellular automaton models for the collective behaviour of the neurons. Consequently, we have studied the ratio $\sigma^2_{\mathrm{Max}}/\sigma^2_{\mathrm{Min}}$ between the maximum and the minimum variance of fluctuations in the excitatory subnetwork as functions of β for a given excitatory probability, α, which coincides with the inhibitory probability, γ. The plausibility of this scenario is suggested by the analysis of the mean-square displacement of EEG signals as performed in Fig. 4. Results are shown in Fig. 6 for several proportions between the number of excitatory and inhibitory neurons. It is remarkable that the maximum value of this ratio is obtained for small values of $\alpha = \gamma$ and only coincides with the experimental ratio in Eq. (25) for a population of inhibitory neurons approximately equal to a 20% of the number of neurons in the excitatory subnetwork. Besides, we also see in Fig. 6 that this ratio could become very large and even diverge as $M \to 0$. This suggests that inhibitory neurons are not only necessary to keep the average excitation of the brain within a certain working regime, but also to apply a brake to fluctuations.

5. Concluding remarks

In this paper we have studied cellular automata with a complete graph topology and stochastic rules as a simple mathematical model for neural dynamics. We have generalised a previous version of the model, in which only excitatory

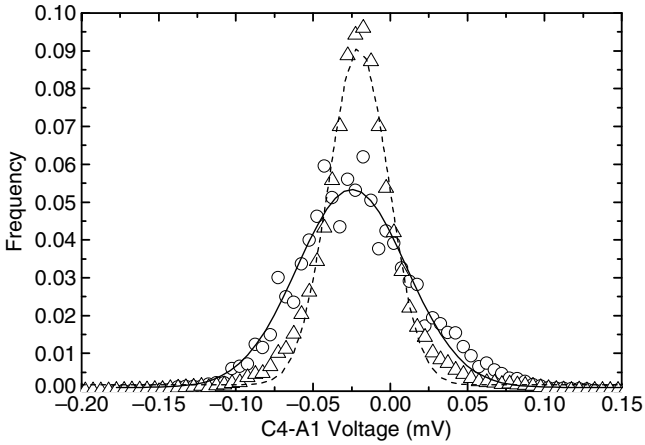

Fig. 5. Histograms of a four minute EEG record for δ rhythm (circles) and a six minute record of α rhythm (triangles). Solid and dashed lines are gaussian fits. The EEG channel was C4-A1 and these records correspond to the same subject.

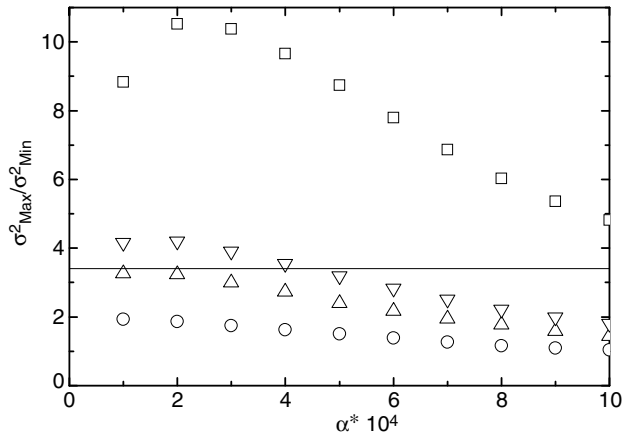

Fig. 6. Ratio between the maximum and the minimum variance of the number of firing neurons in the excitatory subnetwork for $\alpha = \gamma$, $N = 1000$ and and several values of M: $M = 800$, squares, $M = 300$, down triangles, $M = 200$, up triangles, and $M = 100$, circles. This ratio was obtained by varying β as the rest of parameters remain constant. Solid lines correspond to the quotient for the maximum and minimum variance of the EEG of normal subjects.

neurons were considered, to take into account a population of inhibitory neural automata. Our proposal is perhaps the most simple, but nontrivial, cellular automata incorporating the minimum requirements to display interesting behaviour and mimic, to some extent, the collective effects of the dynamics of the real cortex: Boolean automata occupy the vertices of the graph, the edges of this graph are analogous to the synapses, each neuron receives inputs from their excitatory and inhibitory neighbours and changes its state from resting to firing with a probability α for every connection with an excitatory firing neuron. Firing neurons become quiescent with probability γ for every firing inhibitory neuron. Refractoriness is simulated by a probability rate β for the spontaneous deactivation of firing neurons. The complete graph topology has been suggested as an appropriate model for the distribution of compartments in the brain containing roughly the square root of the total number of neurons ($\sim 10^5$) [24]. This seems more realistic than two-dimensional geometries used in previous cellular automata models [12]. The main advantage of discrete cellular automata models is that we can explicitly calculate the fluctuations in the number of firing neurons. Our interest in these fluctuations arises from our hypothesis that electroencephalographic (EEG) records and other global monitoring methods for brain activity (Magnetoencephalograms, Positron emission tomography) should exhibit these fluctuations as a noisy background. The prediction of a gaussian subdiffusive noise is, at least, consistent with the statistical analysis of EEG, if we consider it as a random walk. Moreover, the ratio of the variances between δ and α rhythms is also similar to the ratio of the maximum and the minimum variance in our cellular automata model when the population of inhibitory neurons is, approximately, 20% of that of excitatory ones.

Statistical analysis of EEG has traditionally been restricted to the frequency spectrum and the so-called amplitude [26], which is an unfortunate term for a clearly nonperiodic signal. Our approach could contribute to a better understanding of EEG and the relation between the states of the brain and global activity signals. In this philosophy, recent clinical studies of comatose patients [28] have stressed the importance of EEG as a tool to evaluate the possible recovery from coma: alpha

coma is followed by diffuse delta waves and, finally, theta activity. Our model could accommodate this process in a scenario in which the excitation, inhibition and spontaneous deactivation probabilities vary as the patient recovers.

Present work could develop along the following experimental and theoretical research lines: First, it would be interesting to analyse both pathological and normal EEG with the techniques proposed in this paper using longer records from more subjects. Of particular interest is the study of alpha coma records in order to test the idea that this is the noisy output of a brain with low activity as suggested by our model. Statistical correlations and the mean-shape of a fluctuation [29] are other independent tools from the theory of random walks whose application to EEG could reveal some hidden features. Nevertheless, it is clear that EEG cannot be merely noise and as we move to smaller and smaller scales organised activity should be observed. In order to fill the gap between collective macroscopic models and more realistic microscopic descriptions of neurons, a second step in the modelling of collective fluctuations would be to substitute our simple automata with Hodgkin–Huxley neurons [30,31], that is, to formulate a detailed neural population model. Population models have been studied since the pioneer work of Wilson and Cowan [32] but little attention have been paid to global spontaneous fluctuations, albeit diffusive noise for single neurons being well-known [30]. Further work should disclose if population models also exhibits the main features of cellular automata: second-order phase transitions, and subdiffusive neural dynamics. Work along these lines is in progress and should be published elsewhere.

References

[1] S. Wolfram, Cellular Automata and Complexity, in: Collected Papers, Westview Press, Boulder, CO, USA, 1994.
[2] E. Ahmed, H.N. Agiza, On modeling epidemics including latency, incubation and variable susceptibility, Physica A 253 (1998) 347–352.
[3] M.L. Martins, G. Ceotto, S.G. Alves, C.C.B. Bufon, J.M. Silva, F.F. Laranjeira, A cellular automata model for citrus variegated chlorosis, Physica A 295 (2001) 42–48.
[4] R.M.Z. Dos Santos, Using cellular automata to learn about the immune system, Internat. J. Modern. Phys. C 9 (6) (1998) 793–799.
[5] U. Hershberg, Y. Louzoun, H. Atlan, S. Solomon, HIV time hierarchy: Winning the war while, losing all the battles, Physica A 289 (2001) 178–190.
[6] G.Ch. Sirakoulis, I. Karafyllidis, A. Thanailakis, A cellular automaton model for the effects of population movement and vaccination on epidemic propagation, Ecological Modelling 133 (2000) 209–223.
[7] A. Deutsch, S. Dormann, Cellular Automaton Modeling of Biological Pattern Formation, Birkhäuser Verlag, Basel, Germany, 2004.
[8] P. Bak, K. Chen, C. Tang, A forest-fire model and some thoughts on turbulence, Phys. Lett. A 147 (1990) 297–300.
[9] J.M. Greenberg, S.P. Hastings, Spatial patterns for discrete models of diffusion in excitable media, SIAM J. Appl. Math. 34 (1978) 515.
[10] G. Bub, A. Shrier, L. Glass, Spiral wave generation in heterogeneous excitable media, Phys. Rev. Lett. 88 (2002) 058101.
[11] Y. Bar-Yam, Dynamics of Complex Systems, Addison-Wesley, Reading, MA, 1997.
[12] M.I. Hoffmann, A cellular automaton model based on cortical physiology, Complex Syst. 1 (1987) 187.
[13] M. Tatsuno, Y. Nagai, W. Aizawa, Rule-dynamical approach to Hippocampal network, Neurocomputing 38 (2001) 965–971.
[14] L. Acedo, A second-order phase transition in the complete graph stochastic epidemic model, Physica A 370 (2006) 613–624.
[15] C.M. MCDermott, M.N. Hardy, N.G. Bazan, J.C. Magee, Sleep deprivation-induced alterations in excitatory synaptic transmission in the CA1 region of the rat hippocampus, J. Physiol. 570 (3) (2006) 553–565.
[16] S. Majumdar, B.N. Mallick, Increased levels of tyrosine hydroxylase and glutamic acid decarboxylase in locus coeruleus neurons after rapid eye movement sleep deprivation in rats, Neurosci. Lett. 338 (3) (2003) 193–196.
[17] H. Murck, T. Struttmann, M. Czisch, T. Wetter, A. Steiger, D.P. Auer, Increase in amino acids in the pons after sleep deprivation: A pilot study using proton magnetic resonance spectroscopy, Neuropsychobiology 45 (3) (2002) 120–123.
[18] L. Bettendorff, M. Sallanon-Moulin, M. Touret, P. Wins, I. Margineanu, E. Schoffeniels, Paradoxical sleep deprivation increases the content of glutamate and glutamine in rat cerebral cortex, Sleep 19 (1) (1996) 65–71.
[19] P. Maquet, D. Dive, E. Salmon, B. Sadzot, G. Franco, R. Poirrier, G. Franck, Cerebal glucose utilization during sleep-wake cycle in man determined by positron emission tomography and [18F]-2-fluoro-2 deoxy-D-glucose method, Brain Res. 513 (1990) 136–143.
[20] M. Abeles, Corticonics: Neural Circuits of the Cerebral Cortex, Cambridge University Press, Cambridge, 1991.
[21] S. Havlin, D. Ben-Avraham, Diffusion and Reactions in Fractals and Disordered Systems, Cambridge University Press, Cambridge, 2000.
[22] H.C. Berg, Random Walks in Biology, Princeton University Press, Princeton, NJ, 1983.
[23] D.A. Ratkowsky, Handbook of Non-linear Regression Models, M. Dekker, New York, 1990.
[24] V. Braitenberg, Brain size and number of neurons: An exercise in synthetic neuroanatomy, J. Comput. Neurosci. 10 (2001) 71–77.
[25] M.A.M. de Aguiar, E.M. Rauch, Y. Bar-Yam, Invasion and extinction in the mean field approximation for a spatial Host-Pathogen model, J. Statist. Phys. 114 (2004) 1417–1451.
[26] A.H. Ropper, R.H. Brown, Adams and Victor's Principles of Neurology, McGraw-Hill, New York, 2005.
[27] A.L. Goldberger, L.A.N. Amaral, L. Glass, J.M. Hausdorff, P.Ch. Ivanov, R.G. Mark, J.E. Mietus, G.B. Moody, C.K. Peng, H.E. Stanley, PhysioBank, PhysioToolkit, and Physionet: Components of a new research resource for complex physiologic signals, Circulation 101 (23) (2000) e215–e220.
[28] S. Fossi, A. Amantini, A. Grippo, C. Cossu, N. Boni, F. Pinto, Anoxic-Ischemic alpha coma: Prognostic significance of the incomplete variant, Neurol. Sci. 24 (2003) 397–400.
[29] A. Baldassarri, F. Colaiori, C. Castellano, Average shape of a fluctuation: Universality in excursions of stochastic processes, Phys. Rev. Lett. 90 (2003) 060601.
[30] W.N. Kistler, W. Gerstner, Spiking Neuron Models: Single Neurons, Populations, Plasticity, Cambridge University Press, Cambridge, 2002.
[31] A.L. Hodgkin, A.F. Huxley, A quantitative description of ion currents and its applications to conduction and excitation in nerve membranes, J. Physiot. (Lond.) 117 (1952) 500–544.
[32] H.R. Wilson, J.D. Cowan, A mathematical theory of the functional dynamics of cortical and thalamic nervous tissue, Kybernetik 13 (1973) 55–80.